Journal of Computational and Applied Mathematics 236 (2011) 1354–1369

Contents lists available at SciVerse ScienceDirect

Journal of Computational and Applied Mathematics

journal homepage: www.elsevier.com/locate/cam

The multi-symplectic Fourier pseudospectral method for solving two-dimensional Hamiltonian PDEs

Yaming Chen *, Songhe Song, Huajun Zhu

Department of Mathematics and System Science, Science School, National University of Defense Technology, Changsha, Hunan, 410073, China

ARTICLE INFO

Article history:
Received 26 November 2010
Received in revised form 16 May 2011

Keywords:
Multi-symplectic
Fourier pseudospectral method
Hamiltonian PDE
Zakharov–Kuznetsov equation
Kadomtsev–Petviashvili equation

ABSTRACT

In this paper, the multi-symplectic Fourier pseudospectral (MSFP) method is generalized to solve two-dimensional Hamiltonian PDEs with periodic boundary conditions. Using the Fourier pseudospectral method in the space of the two-dimensional Hamiltonian PDE (2D-HPDE), the semi-discrete system obtained is proved to have semi-discrete multi-symplectic conservation laws and a global symplecticity conservation law. Then, the implicit midpoint rule is employed for time integration to obtain the MSFP method for the 2D-HPDE. The fully discrete multi-symplectic conservation laws are also obtained. In addition, the proposed method is applied to solve the Zakharov–Kuznetsov (ZK) equation and the Kadomtsev–Petviashvili (KP) equation. Numerical experiments on soliton solutions of the ZK equation and the KP equation show the high accuracy and effectiveness of the proposed method.

1. Introduction

It is well known that a large class of PDEs can be written as a Hamiltonian PDE

$$Mz_t + Kz_x = \nabla_z S(z), \tag{1}$$

where $z(x, t) \in \mathbb{R}^n$ $(n \geq 3)$, M and K are skew-symmetric matrices, and $S(z)$ is a smooth Hamiltonian function. These PDEs include the KdV equation [1], nonlinear Schrödinger equation [2–4], Zakharov system [5], Camassa–Holm equation [6,7], and so on. The most important intrinsic property of the Hamiltonian PDE (1) is that it satisfies a multi-symplectic conservation law [8,9]. So it is natural to require a discretization or semi-discretization to preserve this conservation law.

Multi-symplectic methods, which can preserve the multi-symplectic conservation law under appropriate discretizations, have been paid a lot of attention in recent years [10–15]. Bridges and Reich in [8] proposed a multi-symplectic Preissman scheme for Eq. (1) by using the implicit midpoint rule in both space and time directions. Reich in [9] proposed a multi-symplectic Runge–Kutta collocation method for the Hamiltonian wave equations. In [16], Bridges and Reich developed multi-symplectic spectral discretizations on Fourier space for the ZK and shallow water equations. Inspired by the multi-symplectic spectral method, Chen and Qin proposed a multi-symplectic Fourier pseudospectral (MSFP) method for solving the nonlinear Schrödinger equation in real space [17]. In [18], Moore and Reich proposed an explicit Euler box scheme for the Hamiltonian PDEs. Recently, effective multi-symplectic splitting methods were proposed [19,20,3].

The MSFP method is one of the most popular multi-symplectic methods, and has good conservation properties and high accuracy in space. Unlike the multi-symplectic spectral method on Fourier space, the MSFP method is on real space and does not need the passage between Fourier space and physical space. So it is cost-effective as regards computations. As far as we know, the MSFP method has seldom been applied for solving high dimensional PDEs. The only work is that of

* Corresponding author. Tel.: +86 13973154240.
E-mail address: chenym-08@163.com (Y. Chen).

0377-0427/$ – see front matter
doi:10.1016/j.cam.2011.08.023

Chen and Liu in [21], where they developed such a method for the 3 + 1-dimensional Klein–Gordon equation, but they did not present numerical experiments. And the MSFP method has not been applied to solve two-dimensional Hamiltonian PDEs with periodic boundary conditions. For these reasons, this paper is devoted to generalizing the MSFP method to solve the two-dimensional Hamiltonian PDEs, including the ZK equation and the KP equation. In addition, some corresponding numerical experiments are presented to see whether the MSFP method works well for two-dimensional Hamiltonian PDEs.

The rest of this paper is organized as follows. In Section 2, the MSFP method for the two-dimensional Hamiltonian PDE (2D-HPDE) is constructed. In Sections 3 and 4, the proposed MSFP method is applied to the ZK equation and the KP equation respectively. Numerical experiments on the propagation and collision of soliton solutions of the ZK equation and the KP equation are presented in Section 5, and show the effectiveness and high accuracy of the proposed method. Finally, conclusions are drawn in Section 6.

2. The multi-symplectic Fourier pseudospectral method for solving the 2D-HPDE

In this section, we consider the MSFP method for solving the 2D-HPDE

$$Mz_t + Kz_x + Lz_y = \nabla_z S(z) \tag{2}$$

with periodic boundary conditions

$$z(x_L, y, t) = z(x_R, y, t), \qquad z(x, y_L, t) = z(x, y_R, t), \tag{3}$$

where $z(x, y, t) \in \mathbb{R}^n$ $(n \geq 3)$, M, K and L are skew-symmetric matrices, $S(z)$ is a smooth Hamiltonian function, and x_L, x_R, y_L and y_R are constants. Eq. (2) satisfies the multi-symplectic conservation law

$$\omega_t + \kappa_x + \tau_y = 0, \tag{4}$$

where $\omega = \frac{1}{2}dz \wedge Mdz$, $\kappa = \frac{1}{2}dz \wedge Kdz$ and $\tau = \frac{1}{2}dz \wedge Ldz$ are pre-symplectic forms and dz satisfies the first-variation form of Eq. (2) [8].

The crucial step of the Fourier pseudospectral method is to approximate the partial differential operators. From [17], we know that the first-order partial differential operator ∂_x yields the Fourier spectral differential matrix D_1. Here D_1 is an $N \times N$ skew-symmetric matrix with elements

$$(D_1)_{j,s} = \begin{cases} \dfrac{1}{2}(-1)^{j+s}\mu \cot\left(\mu \dfrac{x_j - x_s}{2}\right), & s \neq j, \\ 0, & s = j, \end{cases} \qquad \text{for } j, s = 1, 2, \ldots, N,$$

where $\mu = \frac{2\pi}{L}$, L is the length of the space interval and the even integer N is the number of the equal subintervals. For more details, see [17,22] and references therein.

Now, we generalize the MSFP method to the 2D-HPDE (2) with periodic boundary conditions (3). Dividing the computing domain $[x_L, x_R] \times [y_L, y_R]$ into $N_x \times N_y$ equal cells, we set

$$Z = [z_{1,1}, z_{2,1}, \ldots, z_{N_x,1}, z_{1,2}, z_{2,2}, \ldots, z_{N_x,2}, \ldots, z_{1,N_y}, z_{2,N_y}, \ldots, z_{N_x,N_y}]^{\mathrm{T}},$$

where $z_{i,j}$ is the approximation to $z(x_i, y_j, t)$, N_x and N_y are both even integers. Then we can get that $A_1 Z$ and $A_2 Z$ are the Fourier pseudospectral discretizations of z_x and z_y respectively. Here $A_1 = D_1^x \otimes I_{N_y}$, $A_2 = I_{N_x} \otimes D_1^y$, D_1^x and D_1^y are the $N_x \times N_x$ and $N_y \times N_y$ first-order Fourier spectral differentiation matrices and I_{N_x} and I_{N_y} are the $N_x \times N_x$ and $N_y \times N_y$ identity matrices respectively. $\otimes$ means the Kronecker inner product.

Therefore, using the Fourier pseudospectral method in the space direction of Eq. (2), we can get a semi-discrete system

$$M\frac{d}{dt}z_{k,l} + \sum_{j=1}^{N_x}(D_1^x)_{k,j}Kz_{j,l} + \sum_{j=1}^{N_y}(D_1^y)_{l,j}Lz_{k,j} = \nabla_z S(z_{k,l}), \quad k = 1, 2, \ldots, N_x,\ l = 1, 2, \ldots, N_y. \tag{5}$$

Theorem 1. *The Fourier pseudospectral semi-discretization (5) has $N_x \times N_y$ semi-discrete multi-symplectic conservation laws*

$$\frac{d}{dt}\omega_{k,l} + \sum_{j=1}^{N_x}(D_1^x)_{k,j}\kappa_{j,l} + \sum_{j=1}^{N_y}(D_1^y)_{l,j}\tau_{k,j} = 0, \tag{6}$$

where $\omega_{k,l} = \frac{1}{2}dz_{k,l} \wedge Mdz_{k,l}$, $\kappa_{j,l} = \frac{1}{2}(dz_{k,l} \wedge Kdz_{j,l} + dz_{j,l} \wedge Kdz_{k,l})$, $\tau_{k,j} = \frac{1}{2}(dz_{k,l} \wedge Ldz_{k,j} + dz_{k,j} \wedge Ldz_{k,l})$, $k = 1, 2, \ldots, N_x$, $l = 1, 2, \ldots, N_y$.

Proof. The corresponding variational equation of (5) is

$$M\frac{d}{dt}dz_{k,l}+\sum_{j=1}^{N_x}(D_1^x)_{k,j}Kdz_{j,l}+\sum_{j=1}^{N_y}(D_1^y)_{l,j}Ldz_{k,j}=S_{zz}(z_{k,l})dz_{k,l}. \tag{7}$$

Taking the wedge product with $dz_{k,l}$ on both sides of (7), we obtain

$$\frac{d}{dt}\omega_{k,l}+\sum_{j=1}^{N_x}(D_1^x)_{k,j}\kappa_{j,l}+\sum_{j=1}^{N_y}(D_1^y)_{l,j}\tau_{k,j}=dz_{k,l}\wedge S_{zz}(z_{k,l})dz_{k,l}. \tag{8}$$

Noticing that $S_{zz}(z_{k,l})$ is a skew-symmetric matrix, we arrive at the $N_x\times N_y$ semi-discrete multi-symplectic conservation laws (6). □

Since D_1^x and D_1^y are skew-symmetric, we can sum (6) and obtain the global symplecticity conservation law

$$\frac{d}{dt}\sum_{k=1}^{N_x}\sum_{l=1}^{N_y}\omega_{k,l}=0. \tag{9}$$

Therefore, we should choose a symplectic integration in the time direction of (5) in order to preserve the global symplecticity. Here we apply the implicit midpoint rule and get the MSFP scheme for the 2D-HPDE (2)

$$M\frac{z_{k,l}^{n+1}-z_{k,l}^{n}}{\Delta t}+\sum_{j=1}^{N_x}(D_1^x)_{k,j}Kz_{j,l}^{1/2}+\sum_{j=1}^{N_y}(D_1^y)_{l,j}Lz_{k,j}^{1/2}=\nabla_z S(z_{k,l}^{1/2}), \tag{10}$$

where $z_{k,l}^n$ is the approximation to $z(x_k,y_l,t_n)$, $z_{k,l}^{1/2}=\frac{1}{2}(z_{k,l}^{n+1}+z_{k,l}^n)$ and Δt is the time step.

Theorem 2. *The MSFP scheme (10) has $N_x\times N_y$ fully discrete multi-symplectic conservation laws*

$$\frac{\omega_{k,l}^{n+1}-\omega_{k,l}^{n}}{\Delta t}+\sum_{j=1}^{N_x}(D_1^x)_{k,j}\kappa_{j,l}^{1/2}+\sum_{j=1}^{N_y}(D_1^y)_{l,j}\tau_{k,j}^{1/2}=0, \tag{11}$$

where $\omega_{k,l}^n=\frac{1}{2}dz_{k,l}^n\wedge Mdz_{k,l}^n$, $\kappa_{j,l}^{1/2}=\frac{1}{2}(dz_{k,l}^{1/2}\wedge Kdz_{j,l}^{1/2}+dz_{j,l}^{1/2}\wedge Kdz_{k,l}^{1/2})$, $\tau_{k,j}^{1/2}=\frac{1}{2}(dz_{k,l}^{1/2}\wedge Ldz_{k,j}^{1/2}+dz_{k,j}^{1/2}\wedge Ldz_{k,l}^{1/2})$, $k=1,2,\ldots,N_x$, $l=1,2,\ldots,N_y$.

Proof. The corresponding variational equation of (10) is

$$M\frac{dz_{k,l}^{n+1}-dz_{k,l}^{n}}{\Delta t}+\sum_{j=1}^{N_x}(D_1^x)_{k,j}Kdz_{j,l}^{1/2}+\sum_{j=1}^{N_y}(D_1^y)_{l,j}Ldz_{k,j}^{1/2}=S_{zz}(z_{k,l}^{1/2})dz_{k,l}^{1/2}. \tag{12}$$

Taking the wedge product with $dz_{k,l}^{1/2}$ on both sides of (12) and noticing that

$$dz_{k,l}^{1/2}\wedge M\frac{dz_{k,l}^{n+1}-dz_{k,l}^{n}}{\Delta t}=\frac{\omega_{k,l}^{n+1}-\omega_{k,l}^{n}}{\Delta t},$$

we can obtain

$$\frac{\omega_{k,l}^{n+1}-\omega_{k,l}^{n}}{\Delta t}+\sum_{j=1}^{N_x}(D_1^x)_{k,j}\kappa_{j,l}^{1/2}+\sum_{j=1}^{N_y}(D_1^y)_{l,j}\tau_{k,j}^{1/2}=dz_{k,l}^{1/2}\wedge S_{zz}(z_{k,l}^{1/2})dz_{k,l}^{1/2}. \tag{13}$$

Since $S_{zz}(z_{k,l}^{1/2})$ is a skew-symmetric matrix, we get the $N_x\times N_y$ fully discrete multi-symplectic conservation laws (11). □

In the next two sections, the proposed MSFP method for the 2D-HPDE is applied to solve the ZK equation and the KP equation respectively.

3. The multi-symplectic Fourier pseudospectral method for solving the Zakharov–Kuznetsov equation

In this section, we consider the MSFP method for solving the two-dimensional Zakharov–Kuznetsov equation

$$u_t + (f(u))_x + u_{xxx} + u_{xyy} = 0, \quad f(u) = 3u^2. \tag{14}$$

From [16] we know that this equation can be cast as a 2D-HPDE (2) with

$$z = [p, u, q, \phi, v, w]^{\mathrm{T}}, \qquad S(z) = up - \frac{1}{2}(v^2 + w^2) - F(u), \qquad F'(u) = f(u),$$
$$M = \begin{bmatrix} \mathbf{0} & M_0 \\ -M_0^{\mathrm{T}} & \mathbf{0} \end{bmatrix}, \qquad K = \begin{bmatrix} \mathbf{0} & K_0 \\ -K_0^{\mathrm{T}} & \mathbf{0} \end{bmatrix}, \qquad L = \begin{bmatrix} \mathbf{0} & L_0 \\ -L_0^{\mathrm{T}} & \mathbf{0} \end{bmatrix},$$

where

$$M_0 = \begin{bmatrix} 0 & 0 & 0 \\ 1/2 & 0 & 0 \\ 0 & 0 & 0 \end{bmatrix}, \qquad K_0 = \begin{bmatrix} 1 & 0 & 0 \\ 0 & 1 & 0 \\ 0 & 0 & 1 \end{bmatrix}, \qquad L_0 = \begin{bmatrix} 0 & 0 & 0 \\ 0 & 0 & 1 \\ 0 & -1 & 0 \end{bmatrix}.$$

The corresponding multi-symplectic conservation law for the ZK equation (14) is given by

$$\omega = \frac{1}{2} du \wedge d\phi, \qquad \kappa = dp \wedge d\phi + du \wedge dv + dq \wedge dw, \qquad \tau = du \wedge dw + dv \wedge dq.$$

The 2D-HPDE for the ZK equation (14) can be written as

$$\begin{cases} \phi_x = u, \\ \dfrac{1}{2}\phi_t + v_x + w_y = p - f(u), \\ w_x - v_y = 0, \\ \dfrac{1}{2}u_t + p_x = 0, \\ u_x - q_y = v, \\ q_x + u_y = w. \end{cases} \tag{15}$$

Applying the Fourier pseudospectral method for spatial discretization of (15), we obtain the semi-discrete system

$$\begin{cases} (A_1\Phi)_{(l-1)N_x+k} = u_{k,l}, \\ \dfrac{1}{2}\dfrac{d\phi_{k,l}}{dt} + (A_1V)_{(l-1)N_x+k} + (A_2W)_{(l-1)N_x+k} = p_{k,l} - f(u_{k,l}), \\ (A_1W)_{(l-1)N_x+k} - (A_2V)_{(l-1)N_x+k} = 0, \\ \dfrac{1}{2}\dfrac{du_{k,l}}{dt} + (A_1P)_{(l-1)N_x+k} = 0, \\ (A_1U)_{(l-1)N_x+k} - (A_2Q)_{(l-1)N_x+k} = v_{k,l}, \\ (A_1Q)_{(l-1)N_x+k} + (A_2U)_{(l-1)N_x+k} = w_{k,l}, \end{cases} \tag{16}$$

where A_1 and A_2 are defined in Section 2, and

$$U = [u_{1,1}, u_{2,1}, \ldots, u_{N_x,1}, u_{1,2}, u_{2,2}, \ldots, u_{N_x,2}, \ldots, u_{1,N_y}, u_{2,N_y}, \ldots, u_{N_x,N_y}]^{\mathrm{T}},$$

$\Phi = [\phi_{1,1}, \phi_{2,1}, \ldots, \phi_{N_x,1}, \phi_{1,2}, \phi_{2,2}, \ldots, \phi_{N_x,2}, \ldots, \phi_{1,N_x}, \phi_{2,N_y}, \ldots, \phi_{N_x,N_y}]^{\mathrm{T}}$, etc.

Integrating the system (16) in time by the implicit midpoint rule, we arrive at the MSFP scheme for the ZK equation (14)

$$\begin{cases} (A_1\Phi^{1/2})_{(l-1)N_x+k} = u_{k,l}^{1/2}, \\ \dfrac{1}{2}\dfrac{\phi_{k,l}^{n+1} - \phi_{k,l}^{n}}{\Delta t} + (A_1V^{1/2})_{(l-1)N_x+k} + (A_2W^{1/2})_{(l-1)N_x+k} = p_{k,l}^{1/2} - f(u_{k,l}^{1/2}), \\ (A_1W^{1/2})_{(l-1)N_x+k} - (A_2V^{1/2})_{(l-1)N_x+k} = 0, \\ \dfrac{1}{2}\dfrac{u_{k,l}^{n+1} - u_{k,l}^{n}}{\Delta t} + (A_1P^{1/2})_{(l-1)N_x+k} = 0, \\ (A_1U^{1/2})_{(l-1)N_x+k} - (A_2Q^{1/2})_{(l-1)N_x+k} = v_{k,l}^{1/2}, \\ (A_1Q^{1/2})_{(l-1)N_x+k} + (A_2U^{1/2})_{(l-1)N_x+k} = w_{k,l}^{1/2}, \end{cases} \tag{17}$$

where $u_{k,l}^{1/2} = \frac{1}{2}(u_{k,l}^{n+1} + u_{k,l}^{n})$, $U^{1/2} = \frac{1}{2}(U^{n+1} + U^{n})$, etc.

The scheme (17) can be written in a compact form:

$$\begin{cases} A_1\Phi^{1/2} = U^{1/2}, \\ \frac{1}{2}D_t\Phi^n + A_1V^{1/2} + A_2W^{1/2} = P^{1/2} - \mathbf{f}(U^{1/2}), \\ A_1W^{1/2} - A_2V^{1/2} = 0, \\ \frac{1}{2}D_tU^n + A_1P^{1/2} = 0, \\ A_1U^{1/2} - A_2Q^{1/2} = V^{1/2}, \\ A_1Q^{1/2} + A_2U^{1/2} = W^{1/2}, \end{cases} \tag{18}$$

where D_t is the finite difference operator which satisfies $D_tU^n = \frac{U^{n+1}-U^n}{\Delta t}$, $\mathbf{f}(U^{1/2}) = [f(u^{1/2}_{1,1}), f(u^{1/2}_{2,1}), \ldots, f(u^{1/2}_{N_x,2}), \ldots, f(u^{1/2}_{1,N_y}), f(u^{1/2}_{2,N_y}), \ldots, f(u^{1/2}_{N_x,N_y})]^{\mathrm{T}}$. Assuming that $N_x = N_y$, we notice that $A_1A_2 = A_2A_1$. Therefore, we can eliminate the auxiliary variables p, q, ϕ, v, w to obtain the equivalent scheme for (18)

$$D_tU^{1/2} + (A_1^3 + A_1A_2^2)A_tU^{1/2} = -A_1A_t\mathbf{f}(U^{1/2}), \tag{19}$$

where A_t is the average operator which satisfies $A_tU^n = \frac{U^{n+1}+U^n}{2}$.

As the equations $\phi_x = u$, $w_x - v_y = 0$, $u_x - q_y = v$ and $q_x + u_y = w$ in (15) contain no time derivatives, we can omit the average operator A_t to get more accurate discretizations in (18) [23], namely

$$A_1\Phi^n = U^n, \qquad A_1W^n - A_2V^n = 0, \qquad A_1U^n - A_2Q^n = V^n, \qquad A_1Q^n + A_2U^n = W^n.$$

Then we can get a corresponding two-time-level scheme for the ZK equation:

$$D_tU^n + (A_1^3 + A_1A_2^2)U^{1/2} = -A_1\mathbf{f}(U^{1/2}). \tag{20}$$

In the numerical experiments, we can use the scheme (20) to get the initial values for the second time level of the scheme (19).

4. The multi-symplectic Fourier pseudospectral method for solving the Kadomtsev–Petviashvili equation

In this section, we consider the MSFP method for solving the KP equation

$$(u_t + (f(u))_x + u_{xxx})_x + \sigma u_{yy} = 0, \tag{21}$$

where $f(u) = 3u^2$ and σ is a constant. In the case of $\sigma = -3$, (21) is usually called the KPI equation, whereas for $\sigma = +3$, it is called the KPII equation.

From [24], we notice that the Eq. (21) can be cast as a 2D-HPDE (2) with

$$z = [\phi, v, u, w, p, q, \psi, e, g, h]^{\mathrm{T}}, \qquad S(z) = up + \frac{1}{2}h^2 + \frac{\sigma}{2}w^2 + u^3 - qv - \psi u - gp - ew,$$
$$M = \begin{bmatrix} \mathbf{0} & M_0 \\ -M_0^{\mathrm{T}} & \mathbf{0} \end{bmatrix}, \qquad K = \begin{bmatrix} \mathbf{0} & K_0 \\ -K_0^{\mathrm{T}} & \mathbf{0} \end{bmatrix}, \qquad L = \begin{bmatrix} \mathbf{0} & L_0 \\ -L_0^{\mathrm{T}} & \mathbf{0} \end{bmatrix}.$$

Here,

$$M_0 = \begin{bmatrix} 0 & 0 & 0 & 0 & 0 \\ 0 & 0 & 0 & 1/2 & 0 \\ 0 & 0 & 0 & 0 & 0 \\ 0 & 0 & 0 & 0 & 0 \\ 0 & 0 & 0 & 0 & 0 \end{bmatrix}, \qquad K_0 = \begin{bmatrix} 1 & 0 & 0 & 0 & 0 \\ 0 & 1 & 0 & 0 & 0 \\ 0 & 0 & 0 & 0 & 1 \\ 0 & 0 & 0 & 0 & 0 \\ 0 & 0 & 0 & 0 & 0 \end{bmatrix}, \qquad L_0 = \begin{bmatrix} 0 & 0 & 0 & 0 & 0 \\ 0 & 0 & 1 & 0 & 0 \\ 0 & 0 & 0 & 0 & 0 \\ 0 & 0 & 0 & 0 & 0 \\ 0 & 0 & 0 & 0 & 0 \end{bmatrix}.$$

The corresponding multi-symplectic conservation law for the KP equation (21) is given by

$$\omega = \frac{1}{2}dv \wedge dg, \qquad \kappa = d\phi \wedge dq + dv \wedge d\psi + du \wedge dh, \qquad \tau = dv \wedge de.$$

In addition, the 2D-HPDE for the KP equation (21) can be written as

$$\begin{cases} q_x = 0, \\ \frac{1}{2} g_t + \psi_x + e_y = -q, \\ h_x = p + 3u^2 - \psi, \\ \sigma w - e = 0, \\ u - g = 0, \\ \phi_x = v, \\ v_x = u, \\ v_y = w, \\ \frac{1}{2} v_t = p, \\ u_x = -h. \end{cases} \tag{22}$$

Similarly with the ZK equation in Section 3, applying the Fourier pseudospectral method in space and the implicit midpoint rule in the time direction of (22), we obtain a MSFP scheme for the KP equation (21):

$$\begin{cases} A_1 Q^{1/2} = 0, \\ \frac{1}{2} D_t G^n + A_1 \Psi^{1/2} + A_2 E^{1/2} = -Q^{1/2}, \\ A_1 H^{1/2} = P^{1/2} + 3(U^{1/2})^2 - \Psi^{1/2}, \\ \sigma W^{1/2} - E^{1/2} = 0, \\ U^{1/2} - G^{1/2} = 0, \\ A_1 \Phi^{1/2} = V^{1/2}, \\ A_1 V^{1/2} = U^{1/2}, \\ A_2 V^{1/2} = W^{1/2}, \\ \frac{1}{2} D_t V^n = P^{1/2}, \\ A_1 U^{1/2} = -H^{1/2}. \end{cases} \tag{23}$$

Noticing that when $N_x = N_y$ the equation $A_1 A_2 = A_2 A_1$ is satisfied, we can eliminate the auxiliary variables $\phi, \psi, q, v, w, e, g, h$ to obtain the equivalent scheme of (23):

$$A_1 D_t U^{1/2} + A_1^4 A_t U^{1/2} + \sigma A_2^2 A_t U^{1/2} + 3A_1^2 A_t (U^{1/2})^2 = 0. \tag{24}$$

Since the equations in (22) contain no time derivatives except the equations $\frac{1}{2} g_t + \psi_x + e_y = -q$ and $\frac{1}{2} v_t = p$, we can eliminate the average operator A_t of the corresponding equations to get more accurate discretizations in (23). Then we can obtain a corresponding two-time-level scheme for the KP equation:

$$A_1 D_t U^n + A_1^4 U^{1/2} + \sigma A_2^2 U^{1/2} + 3A_1^2 (U^{1/2})^2 = 0. \tag{25}$$

Like for the ZK equation, we can use the scheme (25) to get the initial values for the second time level of the scheme (24) in the numerical experiments.

5. Numerical experiments

In this section, we present some numerical examples to show the accuracy and effectiveness of the proposed method (19) and (24). For the sake of comparison, we adopt those examples provided in [25], which are integrated by the local discontinuous Galerkin method therein. As we know, local discontinuous Galerkin method is one of the most popular numerical methods for solving PDEs. Many experiments have illustrated its effectiveness [26–30]. In this paper, we use the simple fixed-point iteration method to solve the schemes (19) and (24) at every time step.

5.1. The ZK equation

Example 5.1. The steady progressive wave solution of the ZK equation

$$u_t + uu_x + \varepsilon(u_{xxx} + u_{xyy}) = 0 \tag{26}$$

is of the form [31]

$$u(x, y, t) = 3c \operatorname{sech}^2\left(0.5\sqrt{\frac{c}{\varepsilon}}((x - ct - x_0)\cos\theta + y\sin\theta)\right), \tag{27}$$

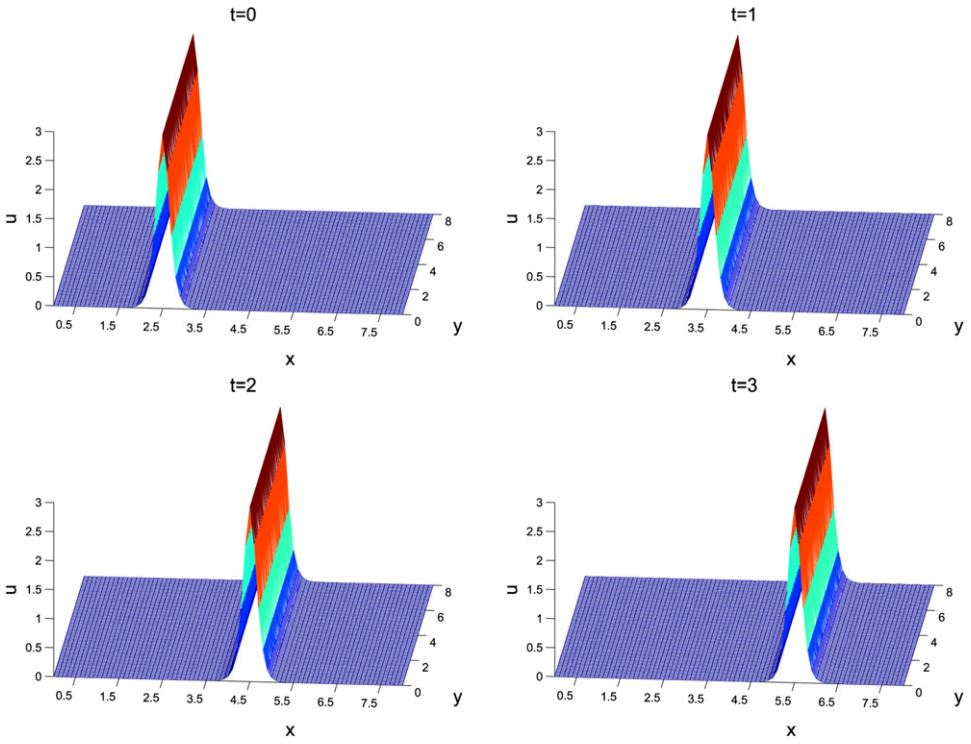

Fig. 1. The propagation of a single line-soliton of the ZK equation (26) with the initial condition (28), using 80×80 uniform cells and time step $\Delta t = 0.001$.

Table 1
The accuracy test of the ZK equation (26) with solution (27) in the space direction, $c = 0.01$, $\varepsilon = 0.01$, $\theta = 0$, $x_0 = 20$ and periodic boundary conditions in $[0, 40] \times [0, 40]$ at time $t = 1$ ($\Delta t = 0.0001$).

$N_x \times N_y$	L^2 error	Order	L^∞ error	Order
10×10	1.47E−03	–	7.28E−05	–
20×20	5.71E−04	1.37	3.09E−05	1.23
40×40	2.34E−05	4.61	1.48E−06	4.38
80×80	1.39E−07	7.40	1.19E−08	6.96

Table 2
Coefficients for the solitary solution (31) of the ZK equation (14).

n	1	2	3	4	5	6	7	8	9	10
a_{2n}	−1.25529873	0.21722635	0.06452543	0.00540862	−0.00332515	−0.00281281	−0.00138352	−0.00070289	−0.00020451	−0.00003053

where θ is an inclined angle with respect to the x-axis, and ε and c are constants. We can see the high accuracy in the space direction of the MSFP method for solving the ZK equation (26) with solution (27) in Table 1.

Example 5.2. We show the propagation and collision of line-solitons of the ZK equation (26) in this example. The case of the propagation of a single line-soliton has the initial condition

$$u(x, y, 0) = 3c \operatorname{sech}^2\left(0.5\sqrt{\frac{c}{\varepsilon}}((x - x_0)\cos\theta + (y - y_0)\sin\theta)\right), \tag{28}$$

where $c = 1$, $\varepsilon = 0.01$, $\theta = 0$, $x_0 = 2.5$, $y_0 = 4$. The case of the collision of double line-solitons has the initial condition

$$u(x, y, 0) = \sum_{j=1}^{2} 3c_j \operatorname{sech}^2\left(0.5\sqrt{\frac{c_j}{\varepsilon}}((x - x_j)\cos\theta + (y - y_j)\sin\theta)\right), \tag{29}$$

where $c_1 = 0.45, c_2 = 0.25, \varepsilon = 0.01, \theta = 0, x_1 = 2.5, y_1 = 0, x_2 = 3.3, y_2 = 0$. The numerical results with periodic boundary conditions in $[0, 8] \times [0, 8]$ are shown in Figs. 1 and 2. From the results, we can see that the

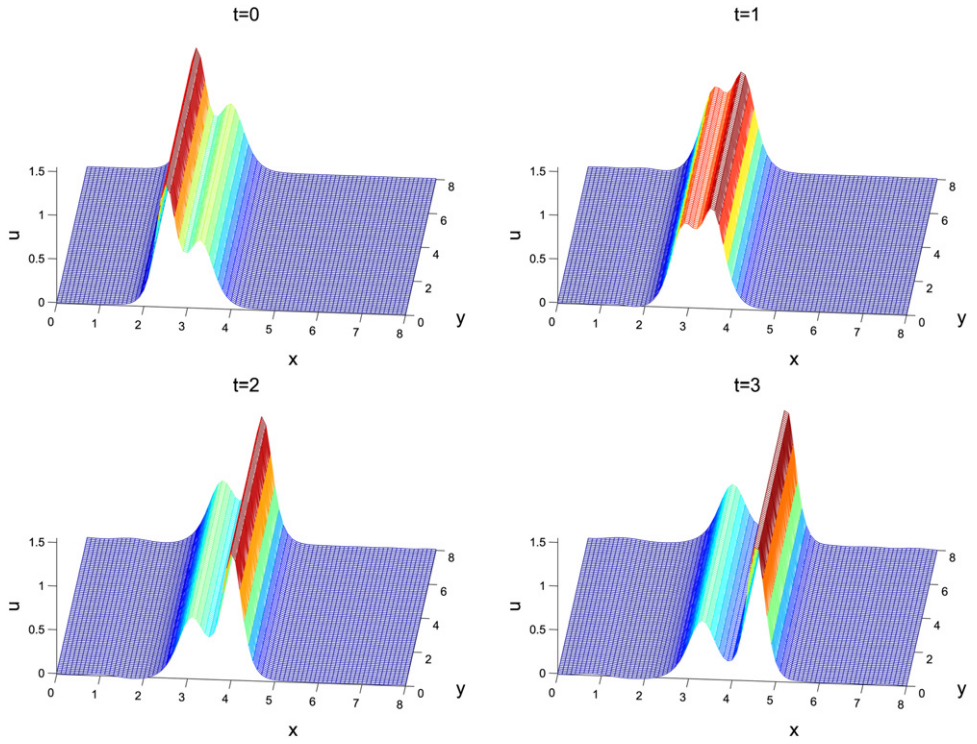

Fig. 2. The collision of two line-solitons of the ZK equation (26) with the initial condition (29), using 80 × 80 uniform cells and time step $\Delta t = 0.001$.

single line-soliton transmits unchanged in the sense of shape and velocity, which is consistent with the exact solution (28). And the collision of double line-solitons is elastic. After collision, the two line-solitons separate from each other and their original shape is restored. These results are similar to those obtained by the discontinuous Galerkin method in [25].

Example 5.3. The ZK equation (14) has a cylindrically symmetric solitary solution [31,32]

$$u(x, y, t) = \frac{c}{3}\sum_{n=1}^{10} a_{2n}\left(\cos\left(2n \operatorname{arccot}\left(\frac{\sqrt{c}}{2}r\right)\right) - 1\right), \tag{30}$$

where c is the velocity of the solitary wave solution and $r = \sqrt{(x - ct)^2 + y^2}$. The coefficients are collected in Table 2. In this example, we show the evolutions and interactions of such solitary solutions. The numerical results for the evolution of a single pulse are shown in Fig. 3 with the initial condition

$$u(x, y, 0) = \frac{c}{3}\sum_{n=1}^{10} a_{2n}\left(\cos\left(2n \operatorname{arccot}\left(\frac{\sqrt{c}}{2}r_0\right)\right) - 1\right), \tag{31}$$

where $c = 4$, $r_0 = \sqrt{(x - x_0)^2 + (y - y_0)^2}$, $x_0 = 10$, $y_0 = 16$. We can see that the pulse transmits with velocity $c = 4$ and without any change in the sense of shape.

Next, we show the results for the collision of two pulses with the initial condition

$$u(x, y, 0) = \sum_{j=1}^{2}\frac{c_j}{3}\sum_{n=1}^{10} a_{2n}\left(\cos\left(2n \operatorname{arccot}\left(\frac{\sqrt{c_j}}{2}r_j\right)\right) - 1\right), \tag{32}$$

where c_1 and c_2 are velocities of solitary wave solutions and $r_1 = \sqrt{(x - x_1)^2 + (y - y_1)^2}$, $r_2 = \sqrt{(x - x_2)^2 + (y - y_2)^2}$. The collisions of two similar pulses are shown in Figs. 4 and 5 with $c_1 = 4.4$ and $c_2 = 4$. Before collision, the velocities of the solitons are preserved better than those obtained in [25]. It is obvious that the two pulses exchanged their amplitudes without merging with each other when collisions happened. This interesting result is consistent with that in [31]. The collisions of two dissimilar pulses are shown in Figs. 6 and 7 with $c_1 = 4$ and $c_2 = 1$. These two figures illustrate that the strong pulse destroys the weak one and generates ripples. The strong pulse seems to

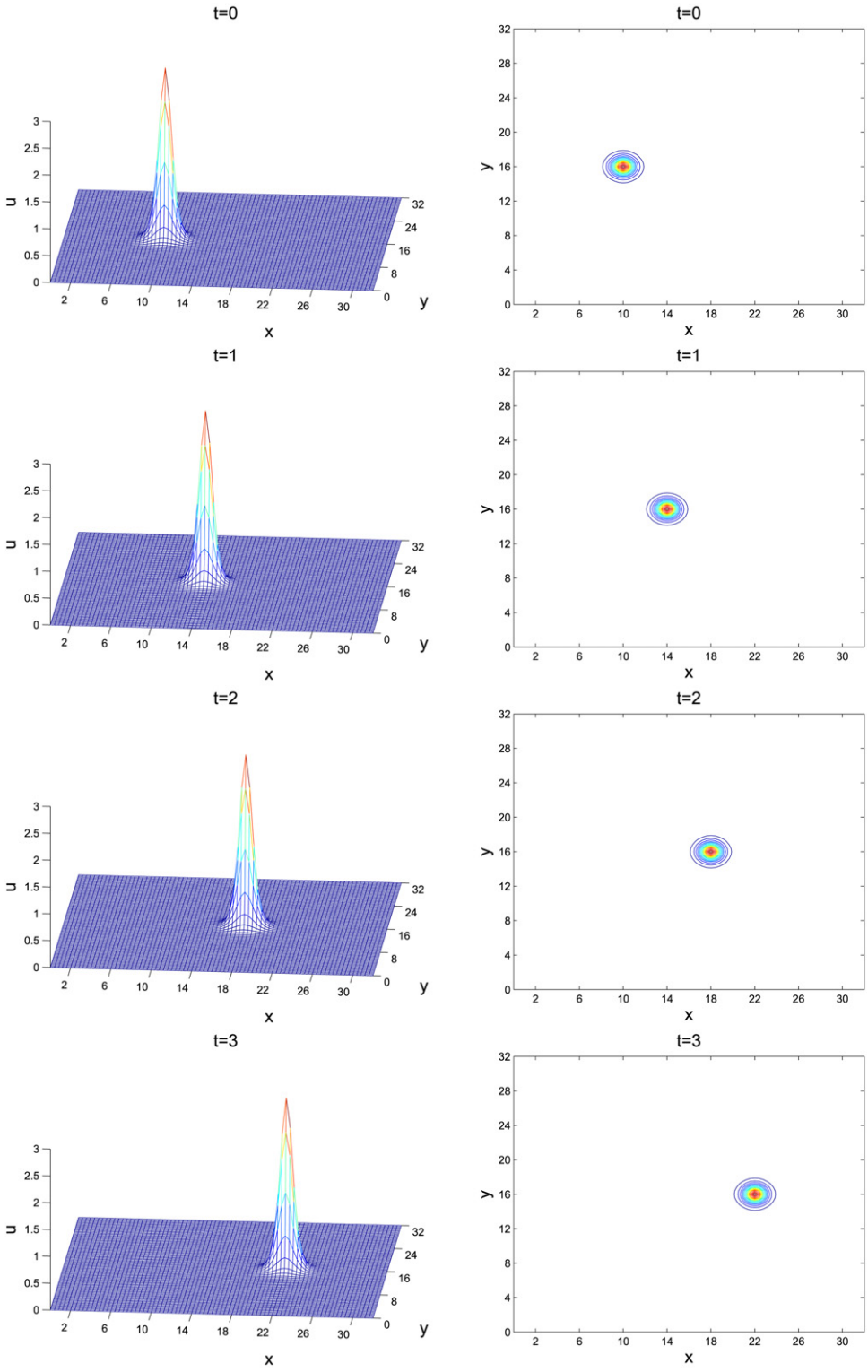

Fig. 3. Evolution of one single pulse solution of the ZK equation (14) with the initial condition (28), using periodic boundary conditions in $[0, 32] \times [0, 32]$ and 80×80 uniform cells ($\Delta t = 0.001$).

recover its cylindrical symmetry after the collision and to propagate stably. The results are similar to that obtained in [31,25].

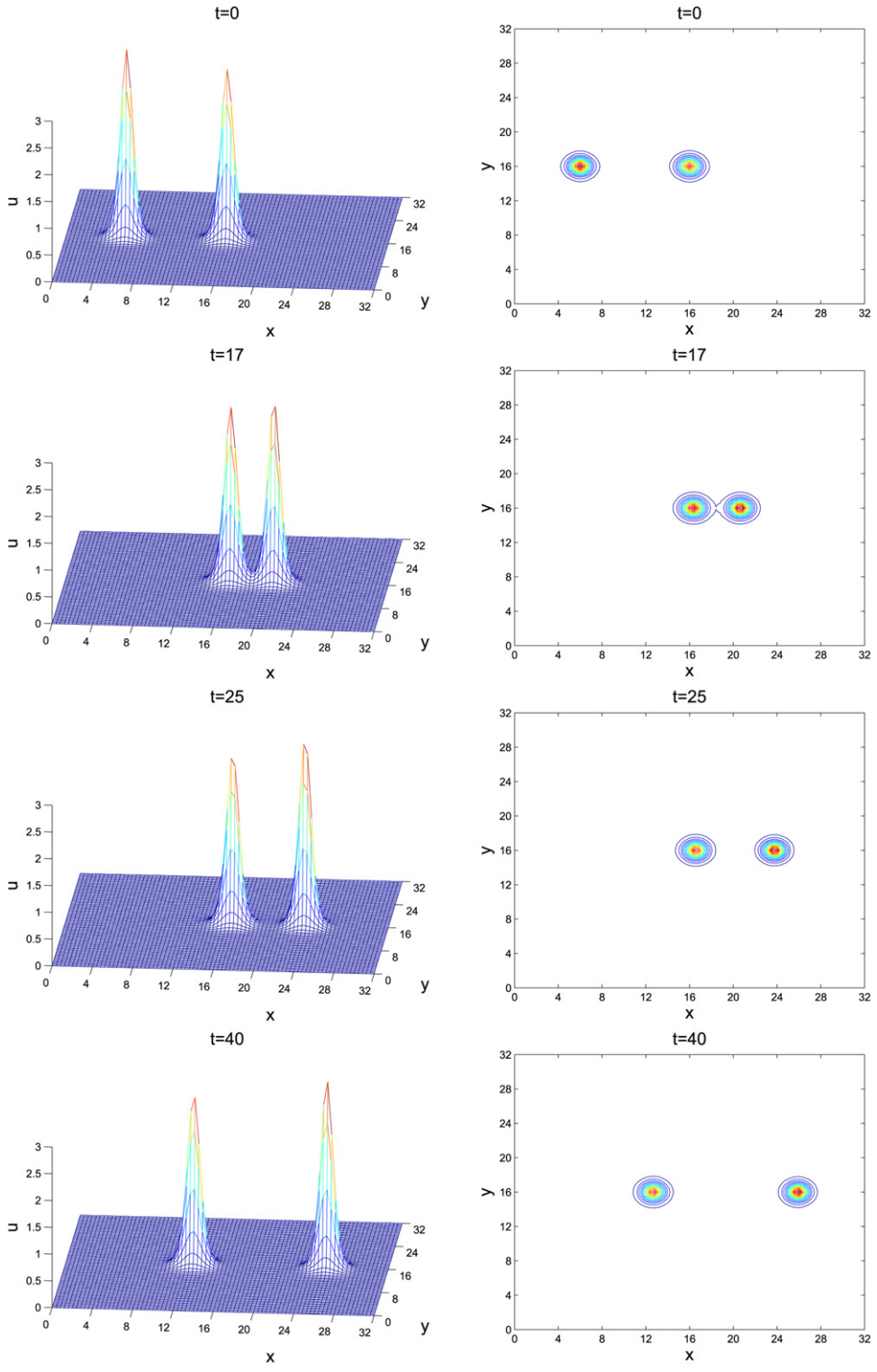

Fig. 4. Solution for the direct collision of two similar pulses of the ZK equation (14) with the initial condition (29), where $x_1 = 6$, $y_1 = 16$, $x_2 = 16$, $y_2 = 16$, using periodic boundary conditions in $[0, 32] \times [0, 32]$ and 80×80 uniform cells ($\Delta t = 0.001$).

5.2. The KP equation

In this subsection, we take the numerical experiments for the KPI equation as the representation of the KP equation.

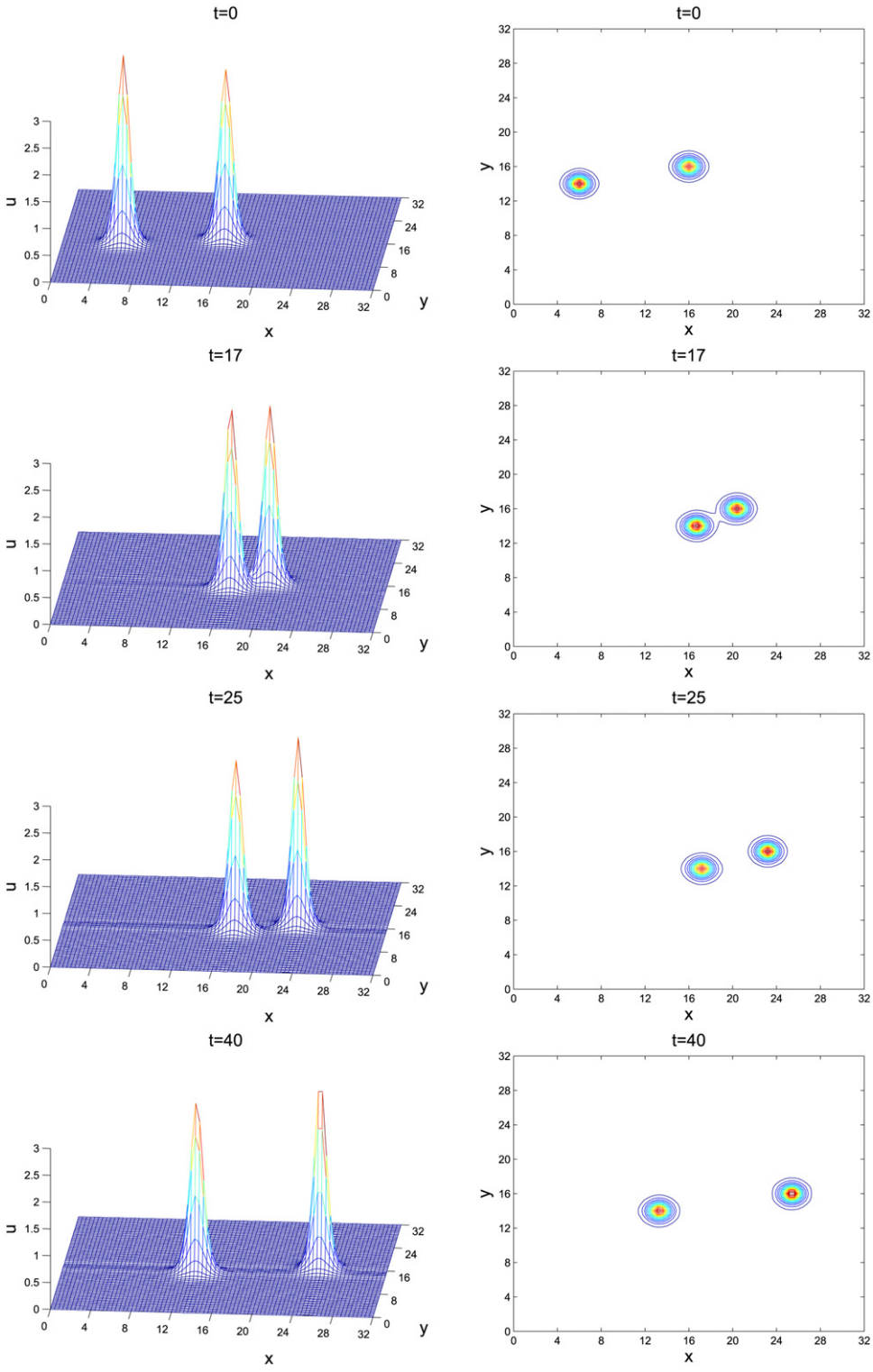

Fig. 5. Solution for the deviated collision of two similar pulses of the ZK equation (14) with the initial condition (29), where $x_1 = 6, y_1 = 14, x_2 = 16, y_2 = 16$, using periodic boundary conditions in $[0, 32] \times [0, 32]$ and 80×80 uniform cells ($\Delta t = 0.001$).

Example 5.4. The KP equation (21) has an exact solution

$$u(x, y, t) = 2k^2 \operatorname{sech}^2(k(x + \lambda y - (4k^2 + \sigma\lambda^2)t - x_0)), \tag{33}$$

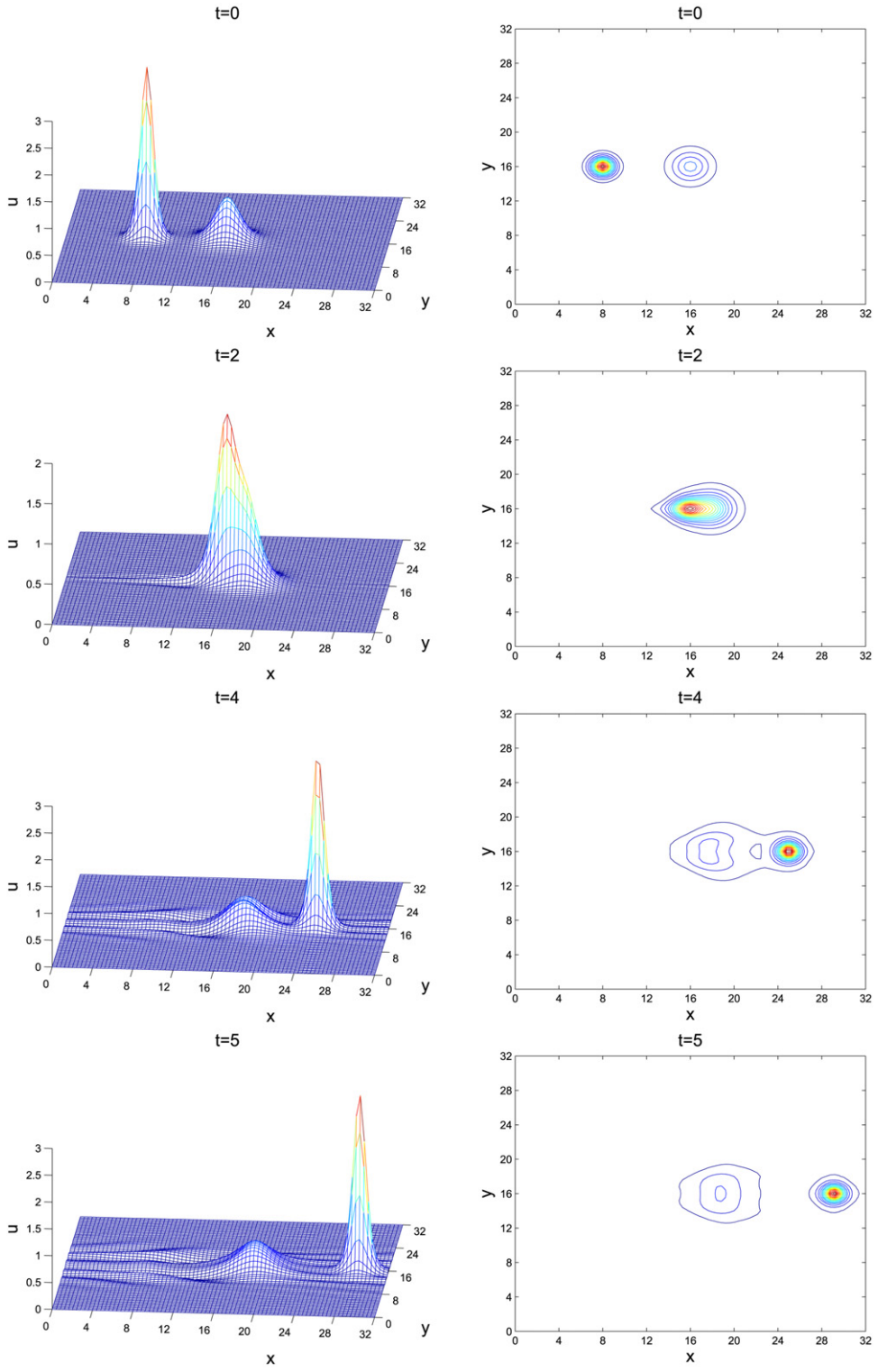

Fig. 6. Solution for the direct collision of two dissimilar pulses of the ZK equation (14) with the initial condition (29), where $x_1 = 8, y_1 = 16, x_2 = 16, y_2 = 16$, using periodic boundary conditions in $[0, 32] \times [0, 32]$ and 80×80 uniform cells ($\Delta t = 0.001$).

where λ, k are constants. This kind of single line-soliton will propagate with the velocity $4k^2 + \sigma\lambda^2$ in the direction at an angle of $\tan^{-1}(-\lambda)^{-1}$ to the positive x-axis. We show an accuracy test of the solution (33) in Table 3, which illustrates the high accuracy of the MSFP method.

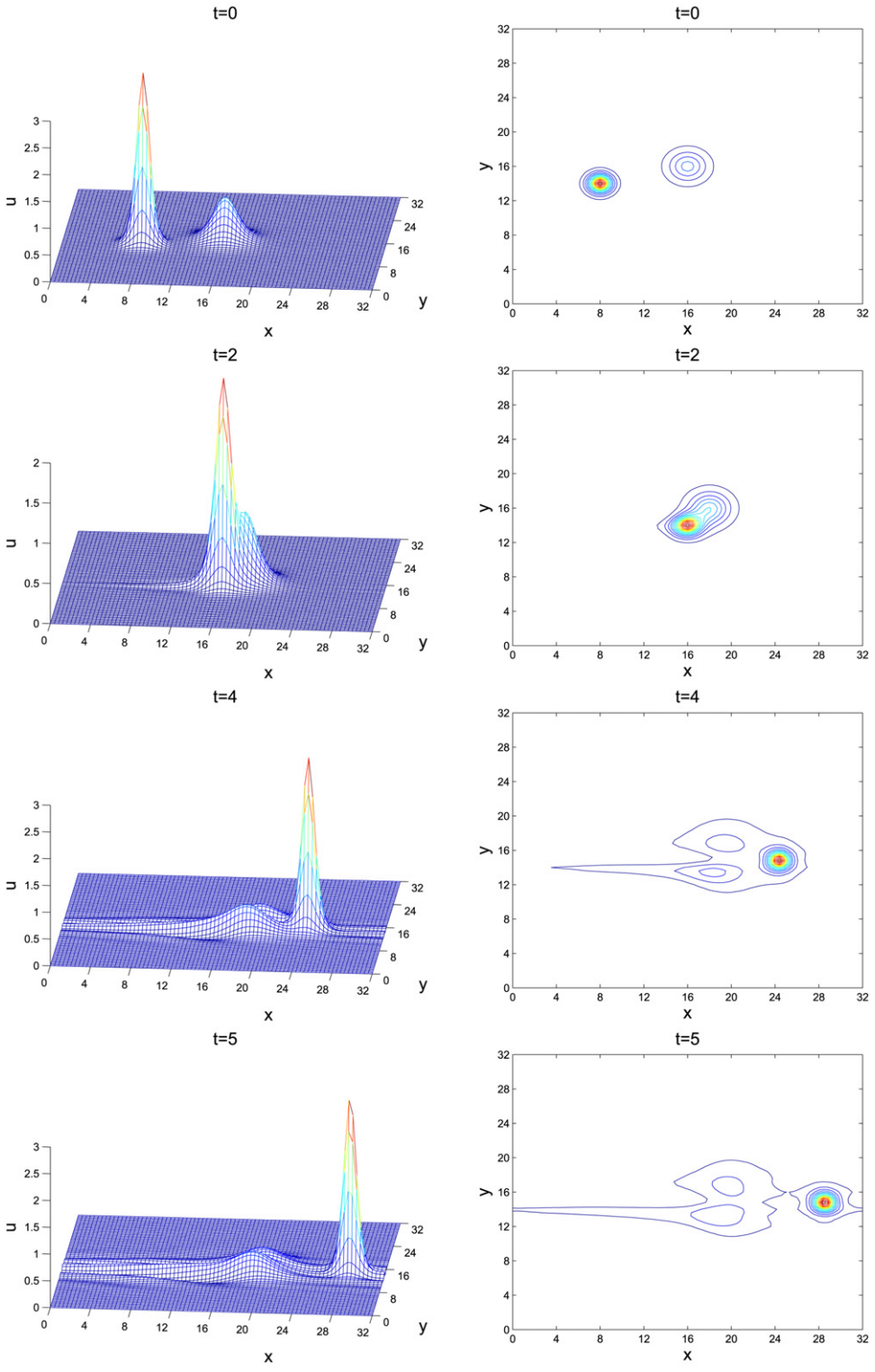

Fig. 7. Solution for the deviated collision of two dissimilar pulses of the ZK equation (14) with the initial condition (29), where $x_1 = 8, y_1 = 14, x_2 = 16, y_2 = 16$, using periodic boundary conditions in $[0, 32] \times [0, 32]$ and 80×80 uniform cells ($\Delta t = 0.001$).

Example 5.5. We show the propagation of one line-soliton of the KPI equation (21) with the initial condition

$$u(x, y, 0) = 2k^2 \mathrm{sech}^2(k(x + \lambda y - x_0)), \tag{34}$$

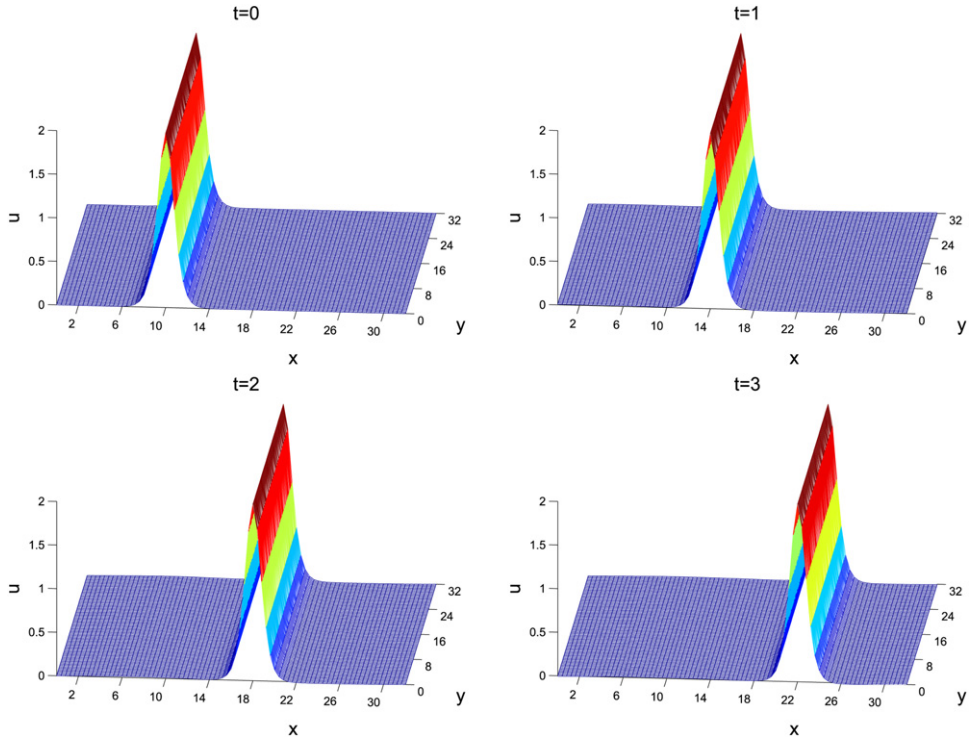

Fig. 8. Propagation of a single line-soliton of the KPI equation (21) with the initial condition (34), using periodic boundary conditions in $[0, 32] \times [0, 32]$ and 80×80 uniform cells ($\Delta t = 0.001$).

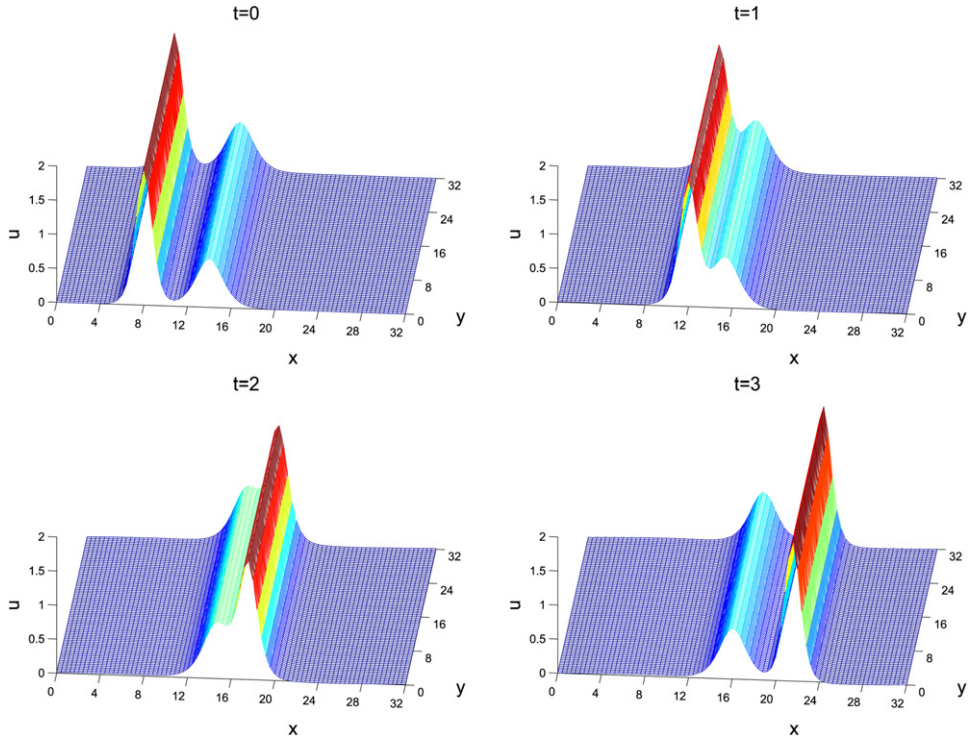

Fig. 9. Collision of two line-solitons of the KPI equation (21) with the initial condition (34), using periodic boundary conditions in $[0, 32] \times [0, 32]$ and 80×80 uniform cells ($\Delta t = 0.001$).

Table 3
The accuracy test of the KPI equation (21) with solution (33) in the space direction, $k = 0.5, \lambda = 0, x_0 = 25$ and periodic boundary conditions in $[0, 50] \times [0, 50]$ at time $t = 0.5$ ($\Delta t = 0.00001$).

$N_x \times N_y$	L^2 error	Order	L^∞ error	Order
20×20	9.39E−01	–	5.73E−02	–
40×40	7.36E−02	3.67	4.98E−03	3.52
80×80	3.25E−05	11.15	9.30E−07	12.39
160×160	2.47E−07	7.04	8.32E−09	6.80

where $k = 1, \lambda = 0, x_0 = 10$. The results are shown in Fig. 8. We can see that the single line-soliton transmits without any change in the sense of shape and velocity.

Moreover, we show the collision of two line-solitons of the KPI equation with the initial condition

$$u(x, y, 0) = 2 \sum_{j=1}^{2} k_j^2 \operatorname{sech}^2(k_j(x + \lambda_j y - x_j)), \tag{35}$$

where $k_1 = 1, k_2 = 0.6, \lambda_1 = 0, \lambda_2 = 0, x_1 = 8, x_2 = 14$. From Fig. 9, we can see that the two line-solitons transmit well before collision. After collision, the two line-solitons separate completely from each other and retain their original shapes.

6. Conclusions

In this paper, we propose a multi-symplectic Fourier pseudospectral method to solve the two-dimensional Hamiltonian PDEs with periodic boundary conditions. Discretizing the two-dimensional Hamiltonian PDE in space by the Fourier pseudospectral method and using the implicit midpoint rule in the time direction, we obtain the multi-symplectic Fourier pseudospectral method for the two-dimensional Hamiltonian PDE. Then, we apply the proposed method to solve the ZK equation and the KP equation. Numerical results show that the proposed method has high accuracy in the space direction and simulates soliton solutions of the ZK equation and the KP equation very well.

Acknowledgments

This work was supported by the Natural Science Foundation of China (No. 10971226), the 973 Project of China (No. 2009CB723802-4), the Research Innovation Fund of Hunan Province (No. CX2011B011) and the Innovation Fund of NUDT (No. B110205).

References

[1] P. Zhao, M. Qin, Multisymplectic geometry and multisymplectic Preissman scheme for the KdV equation, J. Phys. A: Math. Gen. 33 (2000) 3613–3626.
[2] J. Sun, M. Qin, Multi-symplectic methods for the coupled 1D nonlinear Schrödinger system, Comput. Phys. Comm. 155 (2003) 221–235.
[3] Y. Chen, H. Zhu, S. Song, Multi-symplectic splitting method for the coupled nonlinear Schrödinger equation, Comput. Phys. Comm. 181 (2010) 1231–1241.
[4] H. Zhu, Y. Chen, S. Song, H. Hu, Symplectic and multi-symplectic wavelet collocation method for the two-dimensional nonlinear Schrödinger equation, Appl. Numer. Math. 61 (2011) 308–321.
[5] J. Wang, Multisymplectic numerical method for the Zakharov system, Comput. Phys. Comm. 180 (2009) 1063–1071.
[6] D. Cohen, B. Owren, X. Raynaud, Multi-symplectic integration of the Camassa–Holm equation, J. Comput. Phys. 227 (2008) 5492–5512.
[7] H. Zhu, S. Song, Y. Tang, Multi-symplectic wavelet collocation method for the nonlinear Schrödinger equation and the Camassa–Holm equation, Comput. Phys. Comm. 182 (2011) 616–627.
[8] T.J. Bridges, S. Reich, Multi-symplectic integrators: numerical schemes for Hamiltonian PDEs that conserve symplecticity, Phys. Lett. A 284 (2001) 184–193.
[9] S. Reich, Multi-symplectic Runge–Kutta collocation methods for Hamiltonian wave equations, J. Comput. Phys. 157 (2000) 473–499.
[10] T.J. Bridges, S. Reich, Numerical methods for Hamiltonian PDEs, J. Phys. A: Math. Gen. 39 (2006) 5287–5320.
[11] J. Hong, X. Liu, C. Li, Multi-symplectic Runge–Kutta–Nyström methods for nonlinear Schrödinger equations with variable coefficients, J. Comput. Phys. 226 (2007) 1968–1984.
[12] A. Aydın, B. Karasözen, Symplectic and multi-symplectic methods for coupled nonlinear Schrödinger equations with periodic solutions, Comput. Phys. Comm. 117 (2007) 566–583.
[13] J. Wang, On multisymplecticity of sinc–Gauss–Legendre collocation discretization for some Hamiltonian PDEs, Appl. Math. Comput. 199 (2008) 105–121.
[14] C.M. Schober, T.H. Wlodarczyk, Multisymplectic and wave action conservation, Math. Comput. Simul. 80 (2009) 83–90.
[15] J. Sun, M. Qin, H. Wei, D. Dong, Numerical simulations of collision behaviors of optical solitons in birefringent fibres, Commun. Nonlinear Sci. Numer. Simul. 14 (2009) 1259–1266.
[16] T.J. Bridges, S. Reich, Multi-symplectic spectral discretizations for the Zakharov–Kuznetsov and shallow water equations, Physica D 152–153 (2001) 491–504.
[17] J. Chen, M. Qin, Multi-symplectic Fourier pseudospectral method for the nonlinear Schrödinger equation, Electron. Trans. Numer. Anal. 12 (2001) 193–204.
[18] B. Moore, S. Reich, Backward error analysis for multi-symplectic integration methods, Numer. Math. 95 (2003) 625–652.
[19] B.N. Ryland, B.I. McLachlan, J. Frank, On multisymplecticity of partitioned Runge–Kutta and splitting methods, Int. J. Comput. Math. 84 (2007) 847–869.
[20] L. Kong, J. Hong, J. Zang, Splitting multi-symplectic integrators for Maxwell's equation, J. Comput. Phys. 229 (2010) 4259–4278.
[21] J. Chen, Multisymplectic pseudospectral discretizations for (3+1)-dimensional Klein–Gordon equation, Commun. Theor. Phys. 50 (5) (2008) 1052–1054.

[22] J. Wang, A note on multisymplectic Fourier pseudospectral discretization for the nonlinear Schrödinger equation, Appl. Math. Comput. 191 (2007) 31–41.
[23] U.M. Asher, R.I. McLachlan, Multisymplectic box schemes and the Korteweg–de Vries equation, Appl. Numer. Math. 48 (2004) 255–269.
[24] T. Liu, M. Qin, Multisymplectic geometry and multisymplectic Preissman scheme for the KP equation, J. Math. Phys. 43 (2002) 4060–4077.
[25] Y. Xu, C.-W. Shu, Local discontinuous Galerkin methods for two classes of two-dimensional nonlinear wave equations, Physica D 208 (2005) 21–58.
[26] B. Cockburn, C.-W. Shu, The discontinuous Galerkin method for time-dependent convection–diffusion systems, SIAM J. Numer. Anal. 35 (1998) 2440–2463.
[27] J. Yan, C.-W. Shu, A local discontinuous Galerkin method for KdV type equations, SIAM J. Numer. Anal. 40 (2002) 769–791.
[28] J. Yan, C.-W. Shu, Local discontinuous Galerkin methods for partial differential equations with high order derivatives, J. Sci. Comput. 17 (2002) 27–47.
[29] D. Levy, C.-W. Shu, J. Yan, Local discontinuous Galerkin methods for nonlinear dispersive equations, J. Comput. Phys. 196 (2004) 751–772.
[30] Y. Xu, C.-W. Shu, Local discontinuous Galerkin methods for nonlinear Schrödinger equations, J. Comput. Phys. 205 (2005) 72–97.
[31] H. Iwasaki, S. Toh, T. Kawahara, Cylindrical quasi-solitons of the Zakharov–Kuznetsov equation, Physica D 43 (1990) 293–303.
[32] B.F. Feng, T. Kawahara, T. Mitsui, A conservative spectral method for several two-dimensional nonlinear wave equations, J. Comput. Phys. 153 (1999) 467–487.